Comprehensive characterisation of polyphenols in leaves and stems of three anti-dengue virus type-2 active Brazilian *Faramea* species (Rubiaceae) by HPLC-DAD-ESI-MS/MS.

Thiago Wolff, Luis A. Berrueta, Ligia M.M. Valente, Rodolfo S. Barboza, Rômulo L.S. Neris, Iris P. Guimarães-Andrade, Iranaia Assunção-Miranda, Adriana C. Nascimento, Mário Gomes, Blanca Gallo, Carmen Iriondo

Phytochemical Analysis. 2019; 30: 62–72.

DOI: 10.1002/pca.2790

Comprehensive characterization of polyphenols in leaves and stems of three anti-DENV-2 active Brazilian *Faramea* species (Rubiaceae) by HPLC-DAD-ESI-CID-MS/MS

Thiago Wolff[a], Luis A. Berrueta[b,*], Ligia M. M. Valente[a,*], Rodolfo S. Barboza[a], Rômulo S. L. Neris[c], Iris P. Guimarães-Andrade[c], Iranaia Assunção-Miranda[c], Adriana C. Nascimento[a], Mário Gomes[d], Blanca Gallo[b], Carmen Iriondo[e]

[a] Instituto de Química, Universidade Federal do Rio de Janeiro, Av. Athos da Silveira Ramos 149, Centro de Tecnologia, Bl. A, Cidade Universitária, 21941-909, Rio de Janeiro, RJ, Brazil

[b] Departamento de Química Analítica, Facultad de Ciencia y Tecnología, Universidad del País Vasco/Euskal Herriko Unibertsitatea (UPV/EHU), P.O. Box 644, 48080 Bilbao, Spain

[c] Instituto de Microbiologia Paulo Góes, Universidade Federal do Rio de Janeiro, Av. Carlos Chagas Filho 373, Centro de Ciências da Saúde, Bl. I, 21941-902, Rio de Janeiro, RJ, Brazil

[d] Instituto de Pesquisas Jardim Botânico do Rio de Janeiro, R. Jardim Botânico 1008, 22470-180, Rio de Janeiro, Brazil

[e] Departamento de Química Orgánica, Facultad de Ciencia y Tecnología, Universidad del País Vasco/Euskal Herriko Unibertsitatea (UPV/EHU), P.O. Box 644, 48080 Bilbao, Spain

* Corresponding authors: luisangel.berrueta@ehu.es (L.A. Berrueta), valente@iq.ufrj.br (L.M.M. Valente)

Abstract

A comprehensive characterization of polyphenols by online high-performance liquid chromatography with diode array detection coupled to electrospray ionization and triple quadrupole mass spectrometry (HPLC-DAD-ESI-CID-MS/MS) of leaf and stem MeOH extracts from the Brazilian species *Faramea bahiensis*, *F. hyacinthina* and *F. truncata* (Rubiaceae) was performed. Structures have been assigned on the basis of the complementary information obtained from retention time, UV-visible spectra, scan mode MS spectra, and fragmentation patterns in product ion scan MS/MS spectra in different collision energies. The use of the mechanisms and fragmentation patterns established with phenolic standards led to successfully characterize thirty-one phenolic compounds. Flavanone *O*-mono- and diglycosides, flavonol *O*-mono- and diglycosides, flavone *O*-mono-, di- and tri-glycosides and flavone *C*-mono- and diglycosides were identified. Scopoletin, caffeic acid and syringic acid were also detected. The leaves of *F. bahiensis* showed to be the richest in phenolic compounds while the leaves of the other two species presented lower diversity and quantity, especially *F. truncata*. The stems revealed that in general have lower occurrence of these compounds than the leaves. The assay for *in vitro* cytotoxity and DENV serotype 2 (DENV-2) infected hepatocarcinoma cell lineage (HepG2) of the stem extracts showed that *F. hyacinthina* and *F. bahiensis* presented a similar anti-DENV-2 activity to those previously described to their leaves. However, a loss of cytoprotective activity of *F. bahiensis* and a higher cytotoxicity of *F. truncata* relative to those previously described to their leaves was observed.

Keywords: polyphenols, HPLC-DAD-ESI-CID-MS/MS, *Faramea* spp., Rubiaceae, anti-dengue activity, Dengue virus

Chemical compounds studied in this article:

5,3',5'-trihydroxyflavanone-7-*O*-api(1→6)glc (no PubChem CID; IUPAC name (2*S*)-7-[(2*S*,3*R*,4*S*,5*S*,6*R*)-6-[[(2*R*,3*R*,4*R*)-3,4-dihydroxy-4-(hydroxymethyl)oxolan-2-yl]oxymethyl]-3,4,5-trihydroxyoxan-2-yl]oxy-2-(3,5-dihydroxyphenyl)-5-hydroxy-2,3-dihydrochromen-4-one); Nar-7-*O*-api(1→6)glc (PubChem CID: 101254151); Heri-7-*O*-api(1→6)glc (no PubChem CID; IUPAC name (2*S*)-7-[(2*S*,3*R*,4*S*,5*S*,6*R*)-6-[[(2*R*,3*R*,4*R*)-3,4-dihydroxy-4-(hydroxymethyl)oxolan-2-yl]oxymethyl]-3,4,5-trihydroxyoxan-2-yl]oxy-5-hydroxy-2-(4-hydroxy-3-methoxyphenyl)-2,3-dihydrochromen-4-

one); Hes-7-*O*-api(1→6)glc (no PubChem CID; IUPAC name (2*S*)-7-[(2*S*,3*R*,4*S*,5*S*,6*R*)-6-[[(2*R*,3*R*,4*R*)-3,4-dihydroxy-4-(hydroxymethyl)oxolan-2-yl]oxymethyl]-3,4,5-trihydroxyoxan-2-yl]oxy-5-hydroxy-2-(3-hydroxy-4-methoxyphenyl)-2,3-dihydrochromen-4-one); Isk-7-*O*-api(1→6)glc (no PubChem CID; IUPAC name (2*S*)-7-[(2*S*,3*R*,4*S*,5*S*,6*R*)-6-[[(2*R*,3*R*,4*R*)-3,4-dihydroxy-4-(hydroxymethyl)oxolan-2-yl]oxymethyl]-3,4,5-trihydroxyoxan-2-yl]oxy-5-hydroxy-2-(4-methoxyphenyl)-2,3-dihydrochromen-4-one); Lut-7-*O*-api(1→6)glc (PubChem CID: 102316301); Api-7-*O*-api(1→6)glc (PubChem CID: 101926832); Aca-7-*O*-api(1→6)glc (PubChem CID: 10303631); Api-6,8-diC-api (no PubChem CID; IUPAC name 5,7-dihydroxy-2-(4-hydroxyphenyl)-6,8-bis[(2*S*,3*S*,4*R*)-3,4-dihydroxy-4-(hydroxymethyl)oxolan-2-yl]chromen-4-one)

Abbreviations

Nar, naringenin; Eri, eriodictyol; Isk, isosakuranetin; Hes, hesperetin; Heri, homoeriodictyol; Lut, luteolin; Api, apigenin; Aca, Acacetin; Kaem, kaempferol; Que, quercetin; Sco, scopoletin; rha, rhamnoside; hex, hexoside; pent, pentoside; glc, glucoside; rut, rutinoside; FVNN, flavanone; FVN, flavone; FVL, flavonol; CM, coumarin.

1. Introduction

Dengue is a neglected mosquito-borne viral infection appearing in tropical and sub-tropical areas worldwide whose incidence has dramatically increased in the last decades (WHO, Updated in April 2017). The World Health Organization (WHO) estimates that 50-100 million people are infected annually by Dengue Virus (DENV) and more than one-third of global population lives at risk areas of DENV infection (Guo et al., 2017). In Brazil, it is placed among one of the most serious public health issues (Brazilian-Federal-Government, 2017). Currently there is no antiviral drug approved for the routine treatment of dengue patients. Thus, the discovery of drugs that can exert antiviral activity against DENV, without being toxic to the host cell is highly desirable.

The genus *Faramea* Aubl. (Rubiaceae) comprises *ca.* 200 species of shrubs, sub-shrubs or trees distributed throughout the Neotropics from Mexico to northern Argentina with 123 species occurring in Brazil (Jardim and Zappi, 2008). As a part of our ongoing search for potential anti-dengue virus agents, the antiviral activity of the leaf MeOH extracts of the Brazilian species *Faramea bahiensis*, *F. hyacinthina* and *F. truncata* in DENV serotype 2 (DENV-2) infected hepatocarcinoma cell lineage

(HepG2) have been reported (Barboza et al., 2017; Nascimento et al., 2017). The chemical study of these extracts led to the isolation, among other, of flavanone and flavonol glycosides including the common presence of the new antiviral isosakuranetin-7-*O*-ß-D-apiofuranosyl-(1→6)-ß-D-glucopyranoside (**27**) (Barboza et al., 2017; Nascimento et al., 2017). However, fractions generated in these studies showed to be still complex mixtures of phenolic compounds which, due to the low amount and / or similar chromatographic behavior, it was not possible to isolate.

Among the methods for the determination of phenolic compounds without isolation, the most widely used is based on reversed-phase high-performance liquid chromatography (RP-HPLC) coupled to diode array detection (DAD) and mass spectrometry (MS) with atmospheric pressure ionization techniques, i.e., electrospray ionization (ESI) or atmospheric pressure chemical ionization (APcI). With the use of tandem MS technologies (MS/MS) in combination with collision-induced dissociation (CID), a considerable number of structures have been investigated and compared, obtaining fragmentation rules and fragmentation patterns that enable discrimination and identification of a wide range of compounds (Domon and Costello, 1988; Ma et al., 1997; Markham, 1982).

In this paper, aim to complete the study of phenolic compounds in the leaves and to access the presence of these compounds in the stems of those three bioactive *Faramea* spp., a comprehensive characterization by online HPLC-DAD-ESI-CID-MS/MS is reported. The structural information provided led to identify and characterize successfully thirty-one phenolic compounds using the mechanisms and fragmentation patterns established in previous study with phenolic standards (Abad-Garcia et al., 2009). In addition, the *in vitro* non-cytotoxity and anti-DENV-2 effects in HepG2 of the stem MeOH extracts from *F. bahiensis* and *F. hyacinthina* are also reported.

2. Results and discussion

The identification of the phenolic compounds for which standards were available (compound name in bold in Table 1) was carried out by comparing their retention time, UV-visible spectra and mass spectra recorded in MS full scan and MS/MS product ion scan mode using as precursor ion the protonated molecule $[M+H]^+$ and the protonated aglycone $[Y_0]^+$ with those obtained by injecting standards in the same conditions. The identity of other compounds was elucidated using the UV-vis

spectra to assign the phenolic class (Abad-Garcia et al., 2009; Markham, 1982), the MS full scan spectra in positive and negative modes to identify the $[M+H]^+$ and $[M-H]^-$ ions, the MS/MS product ion spectra using the $[M+H]^+$ ion as precursor to assign the protonated aglycone $[Y_0]^+$ and fragmentations observed in both MS/MS product ion spectra using $[M+H]^+$ or $[Y_0]^+$ as precursors to elucidate other structural details (Fig. 1). Additionally, the chromatographic elution order aided in some structural assignments as previously described (Abad-Garcia et al., 2009). Structures and main fragmentation pathways of the studied compounds are presented in Figs. 1 and 2. The thirty-one identified polyphenolic compounds are showed in Table 1.

Figure 1

Figure 2

2.1. Flavanones

2.1.1. Flavanone-O-monoglycoside

One flavanone-*O*-monoglycoside was detected in *F. bahiensis* leaves. ESI(+)-MS/MS product ion spectrum from $[M+H]^+$ (*m/z* 451) showed the ion $[Y_0]^+$ at *m/z* 289 as base peak, resulting from the loss of a residue of hexose. The ESI(+)-MS/MS product ion spectra obtained using as precursor ion the protonated aglycone $[Y_0]^+$ (*m/z* 289) revealed a similar fragmentation pattern to eriodictyol aglycone. The presence of eriodictyol-7-*O*-glucoside (peak **5,** *R*t 52.3) (Table 1) was confirmed by comparison to standard. However, its isomer eriodictyol 5,7,3',5'-tetrahydroxy-flavanone-7-*O*-glucoside has been already characterized by NMR as component of *F. bahiensis* leaves (Nascimento et al., 2017), and it would probably have the same *R*t of **5**.

2.1.2. Flavanone-O-diglycoside

Eriodictyol-7-*O*-rutinoside, isosakuranetin-7-*O*-api(1→6)glucoside, 5,3',5'-trihydroxy-flavanone-7-*O*-api(1→6)glucoside and isosakuranetin-7-*O*-rutinoside standards allowed the identification of these three flavanones in *Faramea* extracts: peaks **8**, *R*t 57.6 min; **27**, *R*t 107.3 min; **6**, *R*t 54.1 min and **29**, *R*t 113.4 min respectively (Table 1).

The bioactive flavanone isosakuranetin-7-*O*-api(1→6)glucoside (**27**) has been already characterized by NMR as component of *F. bahiensis*, *F. truncata* and *F. hyacinthina* leaves (Barboza et al., 2017;

Nascimento et al., 2017). The 5,3',5'-trihydroxy-flavanone-7-*O*-api(1→6)glucoside (**6**), already characterized by NMR (Barboza et al., 2017), was detected in *F. bahiensis* leaves and *F. hyacinthina* leaves and stems. The flavanone-7-*O*-rutinosides: eriodictyol-7-*O*-rutinoside was detected in *F. bahiensis* leaves and stems and isosakuranetin-7-*O*-rutinoside in *F. bahiensis* and *F. truncata* leaves. We also detected other three flavanones that we strongly suggest contain a 7-*O*-ß-D-apiofuranosyl-(1→6)-ß-D-glucopyranoside sugar unit [api(1→6)glucoside].

Peak **13** (*R*t 69.5 min), present in the three studied *Faramea* leaves and *F. hyacinthina* stems, was identified as naringenin-7-*O*-api(1→6)glucoside. This compound showed the same UV spectrum as standard flavanones. The protonated and deprotonated molecular ions detected in MS^1 scan spectra in positive and negative modes were 567 and 565, respectively. The ESI(+)-MS/MS product ion spectrum obtained using as precursor ion the protonated aglycone $[Y_0]^+$ (*m/z* 273) revealed the characteristic fragmentation pattern of naringenin aglycone (Fig. 2, Table 1ESM, Electronic Supplementary Material). The ESI(+)-MS/MS product ion spectrum obtained using as precursor ion the $[M+H]^+$ ion yielded the product ions $[Y_1]^+$, $[Y^*]^+$ and $[Y_0]^+$, which correspond to the losses of apiose, glucose and apiose-glucose residues, respectively, and $[B_1]^+$ and $[B_2]^+$ at *m/z* 133 and 295 (Fig. 1, Table 1ESM). The ion $[Y^*]^+$ has been rationalized by a migration of a hydrogen from C-5-hydroxyl group of the aglycone to terminal apiose and a rearrangement in which the glucose acetal oxygen migrates to terminal apiose anomeric carbon, losing the internal glucose residue, as was also observed for isosakuranetin-7-*O*-api(1→6)glucoside (Fig. 3), and has already been described for rhamnosylglucose sugar unit (Ma et al., 2000). The naringenin-7-*O*-api(1→6)glucoside has been already characterized as component of *F. bahiensis* leaves (Nascimento et al., 2017) and described in species of Piperaceae and Polypodiaceae families (Masuoka et al., 2003). In addition, the aglycone naringenin (peak **28**, *R*t 111.0) was detected in leaves of the three species.

Peak **15** (*R*t 72.5 min), present in *F. bahiensis* leaves, and peak **19** (*R*t 79.2 min), present in *F. bahiensis* and *F. hyacinthina* leaves, were tentatively identified as the isomers homoeriodictyol-7-*O*-api(1→6)glucoside and hesperetin-7-*O*-api(1→6)glucoside, respectively. These compounds showed the same UV spectrum of the standard flavanones, and the same protonated and deprotonated molecular ions at *m/z* 597 and 595 in MS^1 scan spectra in positive and negative modes, respectively.

The ESI(+)-MS/MS product ion spectra obtained using as precursor ion the $[M+H]^+$ ion yielded the product ions $[Y_1]^+$, $[Y^*]^+$ and $[Y_0]^+$ at *m/z* 465, 435 and 303, and $[B_1]^+$ and $[B_2]^+$, characteristic of the glycan sequence (Table 1ESM, Fig. 1). The ESI(+)-MS/MS product ion spectra obtained using as precursor ion the protonated aglycone $[Y_0]^+$ (*m/z* 303) were practically identical and did not give extra data to distinguish between these aglycones (Table 1ESM, Fig. 2). The aglycone identity was determined tentatively as homoeriodictyol due to its earlier elution in relation to its hesperetin isomer (Gil-Izquierdo et al., 2004). To our knowledge these flavanones have not been described before. Other flavanone-7-*O*-ß-D-apiofuranosyl-(1→6)-ß-D-glucopyranosides has been previously described for naringenin, eriodictyol, farrerol and matteucinol (Hori et al., 1988; Masuoka et al., 2003; Takahashi et al., 2001; Zhang et al., 2003).

The presence of flavanone-7-*O*-ß-D-apiofuranosyl-(1→6)-ß-D-glucopyranoside in these *Faramea* species suggests for all compounds the same sugar position and interglycosidic linkage type between glucose and apiose. Moreover, these compounds (peaks **13**, **15** and **19**) eluted at a lower retention time than its corresponding rutinoside, in the same way that the standards isosakuranetin-7-*O*-api(1→6)glucoside (*R*t 107.3 min) and isosakuranetin-7-*O*-rutinoside (*R*t 113.4 min).

Figure 3

2.2. Flavones

2.2.1. Flavone-O-monoglycoside

Apigenin-7-*O*-glucoside (peak **23**, *R*t 88.4 min) was detected in *F. bahiensis* leaves. The MS^1 scan spectra allowed detecting the protonated and deprotonated molecular ions at *m/z* 433 and 431 in positive and negative modes, respectively. The ESI(+)-MS/MS product ion spectrum from the protonated aglycone ($[Y_0]^+$ at *m/z* 271) revealed the characteristic fragmentation pattern of apigenin aglycone. ESI(+)-MS/MS product ion spectrum from $[M+H]^+$ (*m/z* 433) showed the ion $[Y_0]^+$ at *m/z* 271 as base peak, resulting from the loss of a residue of hexose (Table 2ESM, Fig. 2). The identity of peak **23** was confirmed by matching its retention time and UV and MS spectra with those of the standard.

2.2.2. Flavone-O-diglycosides

Apigenin-7-*O*-rutinoside (peak **24a**, *R*t 90.5 min) was identified by comparison with standard. This compound eluted together with **24b**, but MS/MS product ions spectra using each $[M+H]^+$ or $[Y_0]^+$ as precursors allowed to discriminate both.

Luteolin-7-*O*-api(1→6)glucoside (peak **18**, *R*t 75.2 min), apigenin-7-*O*-api(1→6)glucoside (peak **22**, *R*t 87.3 min), chrysoeriol/diosmetin-7-*O*-api(1→6)glucoside (peak **24b**, *R*t 90.5 min) and acacetin-7-*O*-api(1→6)glucoside (peak **30,** *R*t 133.8 min) were detected in *F. bahiensis* leaves. These compounds showed UV spectra characteristic of flavones. MS^2 product ion spectra of $[M+H]^+$ of these compounds at collision energy of 10 eV showed the $[M+H]^+$ ion as base peak and product ions $[Y_1]^+$, $[Y_0]^+$ and $[B_1]^+$ (*m/z* 133), characteristic of the glycan sequence (Table 2ESM, Fig. 2). The aglycones were confirmed by ESI(+)-MS/MS product ion spectra obtained using as precursor ion the protonated aglycone $[Y_0]^+$, but the isomers chysoeriol and diosmetin were not possible to be distinguished. Moreover, these compounds eluted at a higher retention time than their corresponding flavanone in the same way that other flavones (Çalis et al., 2008), suggesting the same sugar position and interglycosidic linkage type for the flavones found in *F. bahiensis*.

Luteolin-7-*O*-api(1→6)glucoside has been previously found in three species of Lamiaceae family, in *Apium graveolens* and in *Cucumis sativus* (Abu-Reidah et al., 2012; Bucar et al., 1988; Çalis et al., 2008; Farooq et al., 1953; La et al., 2015). Chrysoeriol-7-*O*-api(1→6)glucoside has also been identified in *Apium graveolens* (Farooq et al., 1953). Apigenin-7-*O*-api(1→6)glucoside has been isolated from *Crotalaria podocarpa* and *Gonocaryum calleryanum* (Kaneko et al., 1995; Wanjala and Majinda, 1999), and tentatively identified in *Lamiophlomis rotata* (La et al., 2015). Acacetin-7-*O*-api(1→6)glucoside has been isolated from *C. podocarpa* and *Bidens parviflora* (Li et al., 2008; Wanjala and Majinda, 1999), and tentatively identified in *Dryoathyrium boryanum* (Cao et al., 2013). It is the first time these flavones are detected in *Faramea* spp.

2.2.3. Flavone-C-glycosides

In *C*-glycosides, the major fragmentation pathways concern cross-ring cleavages of the saccharide residue and the loss of molecules of water (Fig. 2) (Abad-Garcia et al., 2008; March et al., 2006;

Waridel et al., 2001). This mass spectral behavior was observed for the peaks **4**, **7**, **11**, **14**, **16**, **17**, and **21** at *R*t 44.7, 55.0, 64.7, 71.8, 73.5, 74.2 and 86.2 min, respectively. The molecular mass suggested the presence of mono and di-*C*-glycosides. To date, C-linked sugars have only been found at the C-6 and/or C-8-positions of the flavonoid nucleus (Jay et al., 2006).

2.2.3.1 Flavone-C-monoglycosides

Peaks **11** and **17**, present in *F. bahiensis* leaves, were identified as apigenin-8-*C*-glucoside and apigenin-6-*C*-glucoside. The UV spectra of these compounds showed a typical profile of flavones and the MS^1 spectra revealed high intensity $[M+H]^+$ and $[M-H]^-$ ions at *m/z* 433 and 431, *C*-glycoside characteristic losses of water molecules and $[^{0,2}X]^+$ and $[^{0,1}X]^+$ ions appearing at -120 and -150 *u* from $[M+H]^+$, indicating that they are *C*-hexosides (Table 3ESM). Differentiation between 6-*C*- and 8-*C*-hexoside isomers was accomplished using the ratio of $[^{0,1}X]^+$ and $[^{0,2}X]^+$ ion intensities in the spectra at 40 eV [17]: a $[^{0,1}X]^+/[^{0,2}X]^+$ ratio near to 1:1 for 8-*C*-isomers (peak **11**) and 2:1 for 6-*C*-isomers (peak **17**). Furthermore, the presence of $[^{0,3}X]^+$ ion is diagnostic for 8-*C* isomers , whereas that of $[M+H-4H_2O]^+$ ion is characteristic of 6-*C* isomers (Table 6ESM), and 6-*C* isomers eluted at a higher retention time than 8-*C* isomers (Abad-Garcia et al., 2008). The fragment $[^{0,2}B]^+$ at 121 *u* confirms the apigenin aglycone. Finally, identity was confirmed by comparison with standards.

2.2.3.2 Flavone-C-diglycosides

Apigenin-6,8-di-*C*-glucoside (peak **4)** and acacetin-6,8-di-*C*-glucoside **(**peak **14**) were detected in *F. bahiensis* leaves. Their MS^1 spectra in negative mode exhibit a high intensity $[M-H]^-$ ion, whereas, in the positive mode, the $[M+H]^+$ ion stands out. The same cleavages and losses are observed to these compounds compared to the *C*-monoglycosides: loss of one, two, three and four molecules of water; $[^{0,2}X]^+$, $[^{0,1}X]^+$, $[^{0,4}X\text{-}2H_2O]^+$, $[^{0,3}X]^+$ cleavages and losses of one molecule of formaldehyde and two or three molecules of water, but, as there are two sugar residues, two simultaneous cleavages can occur in both sugars. In this way, many combinations are possible, so the number of fragments is higher. Both diagnostic fragments, $[M+H-4H_2O]^+$ for *C*-6 and $[^{0,3}X]^+$ for *C*-8 are present. The base peak in the spectrum at 20 eV was the $[^{0,2}X\text{-}H_2O]^+$ ion. Since it has been observed very weak (relative abundance < 5) for *C*-monoglycosides, this ion serves as a good diagnostic ion for *C*-diglycosides. Most ions of the spectrum at 40 eV are caused by two simultaneous cleavages occurring in both sugars, but also it is

observed the $[^{0,2}B]^+$ ion at 121 or $[^{0,4}B\text{-}H_2O]^+$ at 159 characterizing the apigenin (peak **4**) and acacetin (peak **14**) aglycone, respectively. MS^2 product ion spectra of $[M\text{-}H]^-$ of these compounds at collision energy of -30 eV showed the $[M\text{-}H]^-$ ion as base peak and loss of -120 and -90 *u* which correspond to the fragments $[^{0,2}X]^-$ and $[^{0,3}X]^-$, respectively (Tables 4ESM and 5ESM, Fig. 2). Finally, identity of apigenin-6,8-*C*-diglucoside (peak **4**) was confirmed by comparison with standard.

Peak **21** was found in *F. bahiensis leaves*. Their MS^1 spectra in positive and negative mode exhibit a high intensity $[M+H]^+$ (*m/z* 535) and $[M\text{-}H]^-$ (*m/z* 533) ions. The MS^2 product ion spectra of $[M+H]^+$ were complex and showed many peaks (Table 4ESM). Both diagnostic fragments $[^{0,1}X]^+$ and $[^{0,4}X]^+$ ions for *C*-glucosides are not appearing at -150 and -60 *u* from $[M+H]^+$ (Fig. 2). The fragments $[M+H\text{-}120]^+$ and $[M+H\text{-}90]^+$ due to $[^{0,1}X]^+$ and $[^{0,2}X]^+$ cleavages for *C*-pentosides and $[^{0,2}B]^+$ at *m/z* 121 for apigenin aglycone were observed (Fig. 2). The $[^{0,3}X]^+$ cleavage has not been detected for *C*-pentosides (Fig. 2). The MS^2 product ion spectrum of $[M\text{-}H]^-$ was simpler than the MS^2 product ion spectrum of $[M+H]^+$. There are not many losses of molecules of water. As the positive fragments, the ions $[M\text{-}H\text{-}120]^-$ and $[M\text{-}H\text{-}90]^-$ due to $[^{0,1}X]^-$ and $[^{0,2}X]^-$ cleavages for *C*-pentosides are observed. In addition, the fragment $[M\text{-}H\text{-}60]^-$ due to $[^{0,3}X]^-$ cleavage have been detected in negative mode (Table 5ESM).

This peak **21** was characterized as apigenin-6,8-*C*-diapioside. Moreover, this compound eluted at a higher retention time than apigenin-6,8-*C*-diglucoside. One flavone described as apigenin- *C*,*C*-dipentosyl has been reported from *Triticum durum* (Cavaliere et al., 2005). Probably unidentified peak D in edible organs of *Sechium edule* (Siciliajo et al., 2004) is the same compound as **21**.

Peaks **7** and **16** were detected in *F. bahiensis* leaves. Their MS^1 spectra in positive and negative mode exhibit high intensity $[M+H]^+$ (*m/z* 565) and $[M\text{-}H]^-$ (*m/z* 563) ions, suggesting to be isomeric *C*-diglycosides. The ESI(+)-MS/MS product ion spectra of both compounds from $[M+H]^+$ showed losses of water and -150, -120, -90 and -60 *u*, characterizing *C*-glucosides and the fragments $[^{0,2}B]^+$ (*m/z* 121) and $[^{0,4}B]^+$ (*m/z* 163) characterizing apigenin aglycone. The difference of $[M+H]^+$ and apigenin-*C*-glucoside is 132 *u*, suggesting the presence of one pentose, and the low intensity of the ion $[M+H\text{-}132]^+$ suggest to be *C*-pentoside. The MS^2 in negative mode product ions -120, -90 and -60 *u* from $[M\text{-}H]^-$ and +113 and +83 from aglycone (Table 5ESM), characterizing *C*,*C*-dipentose-glucoside (Ferreres

et al., 2007; Ferreres et al., 2003). Ferreres et al. (2003) suggest the differentiation of pentose position could be define through the intensity of the ion $[M-H-60]^-$ and retention time, but the intensity of this ion was very similar in our case. So, peak **7** was identified as apigenin-6-*C*-apioside-8-*C*-glucoside because has been eluted at lower retention time than peak **16** that was identified as apigenin-6-*C*-glucoside-8-*C*-apioside. In time, all pentoses founded in this work were characterized as apiose. Injection of apigenin-6-*C*-glucoside-8-*C*-arabinoside (schaftoside) and apigenin-6-*C*-arabinoside-8-*C*-glucoside (isoschaftoside) standards did not match in retention time (59.85 and 72.97 min, respectively) with **7** and **16**, discharging arabinose unit.

Apigenin-6-*C*-apioside-8-*C*-glucoside has been previously found in *Montanoa bipinnatifida* leaves (Khattab and Nada, 2007) and apigenin-6-*C*-glucoside-8-*C*-apioside in *Xanthosoma violaceum* leaves, *Sechium edule* edible organs and aerial parts of *Centaurea deflexa* (Chicca et al., 2011; Picerno et al., 2003; Siciliajo et al., 2004). These are the first reports of flavone-*C*-glycosides in *Faramea* spp.

2.3. Flavonols

2.3.2. Flavonol-O-glycosides

Peak **25** (*R*t 93.5), present in *F. truncata* stems, was identified as kaempferol-3-*O*-glucoside by comparison with standard compound. This compound showed UV spectrum characteristic of flavonol and the ESI(+)-MS/MS product ion spectra obtained using as precursor ion the protonated aglycone $[Y_0]^+$ (*m/z* 287) revealed a similar fragmentation pattern to kaempferol aglycone.

2.3.2. Flavonol-O-diglycosides

Kaempferol-3-*O*-rutinoside (peak **26**, *R*t 94.8 min) was characterized in *F. truncata* and *F. hyancinthina* leaves and stems and quercetin-3-*O*-rutinoside (peak **20**, *R*t 79.6 min) in *F. truncata* stems and *F. hyacinthina* leaves and stems by comparison with reference standard. MS^2 product ions spectra of $[M+H]^+$ ion for these compounds showed $[Y_0]^+$ ion more abundant than the $[Y_1]^+$ ion and a weak $[Y^*]^+$ ion (Table 6ESM).

2.3.3. Flavonol-O-triglycosides

Single stage MS experiments and UV-visible spectra readily lead to the determination of the peaks **9**, **10** and **12** (*R*t 61.3, 62.5 and 68.8 min, respectively) as flavonol triglycosides, which explains their

early elution. On the basis of *m/z* values, these flavonoids should be dihexosyl-rhamnosyl-flavonols (Table 1). MS^2 product ion spectra of $[Y_0]^+$ ion confirm the identity of the aglycones as quercetin (**9**) and kaempferol (**10** and **12**). The glycosylation pattern was tentatively determined by MS^2 product ion spectra of $[M+H]^+$. Peaks **9** and **10** are present in *F. hyacinthina* leaves as well as quercetin-3-*O*-rutinoside and kaempferol-3-*O*-rutinoside, hypothesizing the presence of a 3-*O*-rutinoside plus one glucose in undefined position. The peak **12**, present in *F. truncata* stems, is an isomer of **10**. The ESI(+)-MS/MS product ion spectra obtained using as precursor ion the $[M+H]^+$ ion yielded the product ions: $[M+H\text{-rham}]^+$, $[M+H\text{-hex}]^+$, $[M+H\text{-rham-hex}]^+$, $[M+H\text{-2hex}]^+$ and $[Y_0]^+$. The ions $[B_1]^+$ and $[B_2]^+$ at *m/z* 147 and 309, respectively, suggest the presence of rutinose. All these facts suggest that these flavonoids are *O*-rutinoside-*O*-glucosides. The identity of peak **9** was confirmed by matching the retention time with quercetin-3-*O*-rutinoside-4'-*O*-glucoside standard, but it was not possible to know the sugar positions of the peaks **10** and **12** (Table 7ESM).

2.4. Other class of phenolics

Caffeic acid (peak **1**, *R*t 24.3 min), syringic acid (peak **2**, *R*t 26.9 min) and scopoletin (peak **3**, *R*t 39.8 min) standards allowed the identification of these three compounds in *Faramea* extracts (Table 1). Caffeic acid is present in *F. bahiensis* stems and *F. hyacinthina* leaves. Syringic acid was detected in all studied extracts but in *F. hyacinthina* leaves, and the coumarin scopoletin, in *F. truncata* and *F. hyacinthina* stems.

2.5. Quantification of polyphenolic compounds

All identified compounds were quantified using a standard for each class. The leaves of *F. bahiensis* showed to be the richest in phenolic compounds while the leaves of the other two species presented lower diversity and quantity, especially *F. truncata* (Table 1). The stems showed in general low occurrence of these compounds. The leaf extracts contain much higher concentration of the bioactive flavanone **27** than do the stem extracts.

Table 1

Figure 4

2.6. Anti-dengue assay

The stem MeOH extracts of the three studied *Faramea* species were assayed for *in vitro* cytotoxic and anti-DENV-2 effects in HepG2. Cell viability assay shows that HepG2 cells present a reduction of 22% on viability 48 h post DENV infection in untreated condition (Fig. 5A). Treatment with 50 µg/ml of MeOH extract of *F hyacintina* stems significantly decreases the effects of DENV infection on cell viability without proliferative effect (Fig. 5A). Treatment with the same dose of *F truncata* stem extract resulted in loss of cell viability, which prevented the assessment of its anti-DENV activity. We did not observe cytoprotection or cytotoxicity with the treatment with the stem extract of *F bahiensis*, thus we included both *F. hyacinthina* and *F. bahiensis* extracts in the viral load analysis. Quantification of DENV particles in culture medium of infected HepG2 by plaque assay demonstrated a significant reduction of the infectious DENV-2 particles when treated with *F hyacintina* (Fig. 5B). Treatment with *F bahiensis* also promotes a reduction on viral load, even without inducing an apparent cytoprotective effect. These results indicate that both stem extracts present an anti-dengue activity, as previously described for the extracts of their leaves (Barboza et al., 2017; Nascimento et al., 2017).

Figure 5

3. Conclusions

The structural information provided by online HPLC-DAD-ESI-CID-MS/MS scan and product ion scan modes led to identify and characterize successfully thirty-one phenolic compounds in the leaf and stem MeOH extracts from the three studied Brazilian *Faramea* spp. using the mechanisms and fragmentation patterns established in previous study with phenolic standards. There are flavanones in all leaf extracts, but flavonols have not been detected in *F. bahiensis* that has the major variety of flavones. Some of the characterized flavonoids have not been described yet and others are for the first time in species of the genus *Faramea*. Scopoletin, caffeic acid and syringic acid were also detected. The stems of *F. hyacinthina* and *F. bahiensis* presented a similar anti-DENV-2 activity to those previously described to their leaves (Barboza et al., 2017). However, a loss of cytoprotective activity of *F. bahiensis* and a higher cytotoxicity of *F. truncata* relative to those previously described to their leaves (Barboza et al., 2017; Nascimento et al., 2017) was observed. The bioactive flavanone

isosakuranetin-7-*O*-ß-D-apiofuranosyl-(1→6)-ß-D-glucopyranoside (**27**) was found in the three species. Although compound **27** may be playing an important role in the activity of *F. bahiensis* and *F. hyacinthina* leaves, it was not possible to establish a relationship between the polyphenolic profiles and the anti-dengue effects of leaves and stems of the three species. Other compounds than polyphenols and/or differences in the cytotoxicity of the individual polyphenolic compounds seem to contribute to the observed activity and cytotoxicity behaviours.

4. Experimental

4.1. Reagents, solvents and standard phenolics

Methanol (MeOH) and dimethyl sulfoxide (DMSO) HPLC grade were supplied by Romil, Chemical Ltd, Heidelberg, Germany. Water was purified on a Milli-Q system (Millipore, Bedford, MA, USA). Glacial acetic acid analytical grade was provided by Merck (Darmstadt, Germany). All solvents used were previously filtered through 0.45 μm nylon membranes (Lida, Kenosha, WI, USA).

Phenolics standards were supplied as follows: eriodictyol-7-*O*-glucoside, eriodictyol-7-*O*-rutinoside, eriodictyol-7-*O*-neohesperidoside, naringenin-7-*O*-rutinoside, hesperetin-7-*O*-rutinoside, hesperetin-7-*O*-neohesperidoside, isosakuranetin-7-*O*-rutinoside, isosakuranetin-7-*O*-neohesperidoside, quercetin-3-*O*-galactoside, kaempferol-3-*O*-glucoside, kaempferol-3-*O*-rutinoside, kaempferol-7-*O*-neohesperidoside, kaempferol-3-*O*-robinoside-7-*O*-rhamnoside, isorhamnetin-3-*O*-glucoside, scopoletin, apigenin-7-*O*-glucoside, apigenin-7-*O*-rutinoside, apigenin-6-*C*-glucoside, apigenin-8-*C*-glucoside, luteolin-7-*O*-glucoside, chrysoeriol, diosmetin,(+) catechin and esculin from Extrasynthèse (Genay, France); while caffeic acid, quercetin dehydrated and quercetin-3- *O*-rutinoside were provided by Sigma-Aldrich Chemie (Steinheim, Germany); quercetin-3-*O*-glucoside by Chromadex (Santa Ana, CA, USA); apigenin-6,8-di-*C*-glucoside, apigenin-6-*C*-glucoside-8-*C*-arabinoside and apigenin-6-*C*-arabinoside-8-*C*-glucoside by Carbosynth (Berkshire, UK); and syringc acid by Fluka Chemie (Steinheim, Germany) Isosakuranentin-7-*O*-apioglucoside, naringenin-7-*O*-apioglucoside and 5,3',5'-trihydroxy-flavanone-7-*O*-apioglucoside were isolated from *F. hyacinthina* leaves and characterized by NMR (Barboza et al., 2017).

All stock standard solutions (in concentrations ranging from 300 to 2700 μg/ml, depending on each phenolic compound) were prepared in MeOH, except for all flavanones and luteolin-7-*O*-glucoside that were dissolved with MeOH-*N*,*N*-dimethylformamide (DMF) (80:20, v/v). All were stored at 4 ºC in darkness.

4.2. Plant material

The species *Faramea bahiensis* was collected at the Restinga de Marambaia, Rio de Janeiro, RJ, Brazil. The species *Faramea truncata* was collected at the Parque Nacional da Serra dos Órgãos, Guapimirim, RJ, Brazil. The species *Faramea hyacinthina* was collected at the Parque Nacional de Itatiaia, Itatiaia, RJ, Brazil. Their voucher specimens were deposited at the Herbarium of the Instituto de Biologia of the Universidade Federal do Rio de Janeiro, RJ, Brazil, under number RFA 37489, RFA 40642 and RFA 40654, respectively. The collection had previous permission from SISBIO-ICMBio-MMA-Brazil under number 46504-2.

4.3. Extraction procedures

The leaves and stems were dried at 40ºC for 24 h. Dried and sieved leaves of *F. bahiensis* (151 g), *F. truncata* (183 g) and *F. hyacinthina* (104 g) were exhaustively and sonically extracted with MeOH. The MeOH was removed under low pressure to yield 7.8 g, 18.7 g and 12.0 g of crude extracts respectively (Barboza et al., 2017). 50 g of dried and sieved stems of each species were extracted with 250 ml of MeOH with ultra-sound assistance at room temp by 15 min (5x). The supernatants were pooled, and the solvents removed under low pressure to yield 1.5 g (*F. bahiensis*), 1.0 g (*F. truncata*) and 2.7 g (*F. hyacinthina*) of crude extracts.

4.4. HepG2 infection and treatment

Human hepatocarcinoma cell lineage (HepG2) cells were grown in Dulbecco's modified Eagle's medium (DMEM) (LGC Biotecnologia) supplemented with 10% fetal bovine serum (FBS), at 37 °C, in an atmosphere of 5% CO_2. HepG2 cells were infected with DENV-2 (strain 16681) in M.O.I. of 1 for 1 h at 37°C in 5% CO_2. After infection, the medium was replaced by fresh medium (DMEM with 5% FBS) with or without 50 μg/ml (in DMSO) of the stem MeOH extracts of *Faramea* spp and

cultured at 37°C in 5% CO_2. The samples (stock 100 µg/µl) were added to the medium (DMEM with 5% FBS) to obtain the desired concentration. The final concentration of DMSO in HepG2 culture was 0.05%, which was also added to the infected and untreated condition. After 48 h of infection, the culture medium was collected for virus quantification by plaque assay and cellular extracts were used to determine viability (as described below).

4.5. Cell Viability Assay

The effect of the MeOH extract of the *Faramea* species stems in infected HepG2 cell viability was determined by measuring the metabolization of 3-(4,5-dimethylthiazol-2-yl)-2,5-diphenyl tetrazolium bromide (MTT metabolization assay) by the cells. Cells seeded in a 24-well plate were infected with DENV-2 and treated as previously described. Cytotoxicity and/or proliferative effects were assessed treating uninfected HepG2 cells in the same conditions. Forty-eight hpi cells were washed with balanced salt solution (BSS) prior to the addition of 500 µl of 0.5 mg/ml MTT (Sigma-Aldrich Co.) in BSS to each well. After 1 h, MTT solution was discarded and the formazan crystals formed were solubilized in each well using 500 µl of 0.04 M HCl solution in *iso*-propanol (*iso*-PrOH). The optical density (OD) of the samples was read at 570 nm and 650 nm for background correction.

4.6. Virus quantification

The virus titer in the culture medium of infected HepG2 cells was quantified by plaque assay in Baby Hamster Kidney cells (BHK-21 cells). Briefly, BHK-21 cells were grown in Minimum Essential Medium (MEM) α (Invitrogen) supplemented with 10% FSB and seeded in 24-well plates and cultured overnight at 37°C with 5% CO_2. Ten-fold serial dilutions of the samples were performed using α-MEM and used to infect BHK-21 cells at 37°C for 1 h. After this period, 1% carboxymethyl cellulose in α-MEM with 2% FBS was added and the cells were kept in culture at 37°C with 5% CO_2 for five days. Then, the cells were fixed with formaldehyde 4% and the plaque was visualized by staining with crystal violet (1% crystal violet powder (w/v), 20% MeOH and H_2O).

4.7. Analytical procedure

4.7.1. Solvent extraction of freeze-dried samples and RP-HPLC

The samples were dissolved in H_2O-MeOH-acid acetic (AcOH) (69:30,1, v/v) yielding solution concentrations ranging from 2.0 to 6.0 mg/ml, depending on each crude extract. The HPLC system was a Waters (Milford, USA) Alliance 2695 coupled to a Waters 2996 DAD. A reversed-phase Phenomenex (Torrance, USA) Luna C18(2) column (150 x 4.6 mm i.d. and particle size 3 µm) with a Waters Nova-Pack C18 guard column (10 x 3.9 mm i.d, 4 µm) was used. A previously reported gradient program was employed (Ma et al., 2000).

4.7.2. Mass spectrometry

Mass spectra were obtained on a Micromass (Milford, MA, USA) Quattro micro triple quadrupole mass spectrometer coupled to the exit of the diode array detector and equipped with a Z-spray ESI source. A flow of 70 µl/min from the DAD eluent was directed to the ESI interface using a flow-splitter. Nitrogen was used as desolvation gas, at 300ºC and a flow rate of 450 L/hr, and no cone gas was used. A potential of 3.2 kV was used on the capillary for positive ion mode and 2.6 kV for negative ion mode. The source block temperature was held at 120 ºC.

MS full scan spectra, within the m/z range 50-1000, were performed in the positive mode at different cone voltages (15, 30 and 45 V) and in the negative mode at -30 V. MS/MS product ion spectra in positive and negative modes were recorded using argon as collision gas at $1.5 \cdot 10^{-3}$ mbar and under different collision energies in the range 10-40 eV and -30 V (for negative) and optimized (for positive polarity) cone voltages. The optimum cone voltages were those which produced the maximum intensity for protonated molecule $[M+H]^+$ and protonated aglycone ion $[Y_0]^+$ in the previous MS experiments.

The nomenclature adopted to denote the fragment ions for glycoconjugates was proposed by Domon and Costello (Domon and Costello, 1988) (Fig. 1). The flavonoid aglycone fragment ions have been designed according to the nomenclature proposed by Ma *et al*. (Ma et al., 1997) (Fig. 2).

4.7.3. Quantitation of phenolic compounds

Quantitation was performed using integration areas in the calibration regression of the standards most similar to each phenolic compound quantified. Thus, flavanones were quantified as eriodictyol-7-*O*-

rutinoside at 280 nm; flavones as apigenin-7-*O*-glucoside at 340 nm; flavonols as quercetin-3-*O*-glucoside at 340 nm; coumarins as scopoletin at 340 nm; hydroxycinnamic acids as caffeic acid at 320 nm; benzoic acids as syringic acid at 280 nm. The concentrations ranged from 0.1 to 150.0 ppm.

Conflict of interest

The authors declare no conflict of interest.

Acknowledgments

The authors thank Fundação Carlos Chagas Filho de Amparo à Pesquisa do Estado do Rio de Janeiro (FAPERJ-Brazil) (Proc. No E-26/111.373/2014) for grant support. A.C.N. thanks CNPq-Brazil and T.W. FAPERJ for fellowships.

Appendix A. Supplementary data

Supplementary data associated with this article can be found at

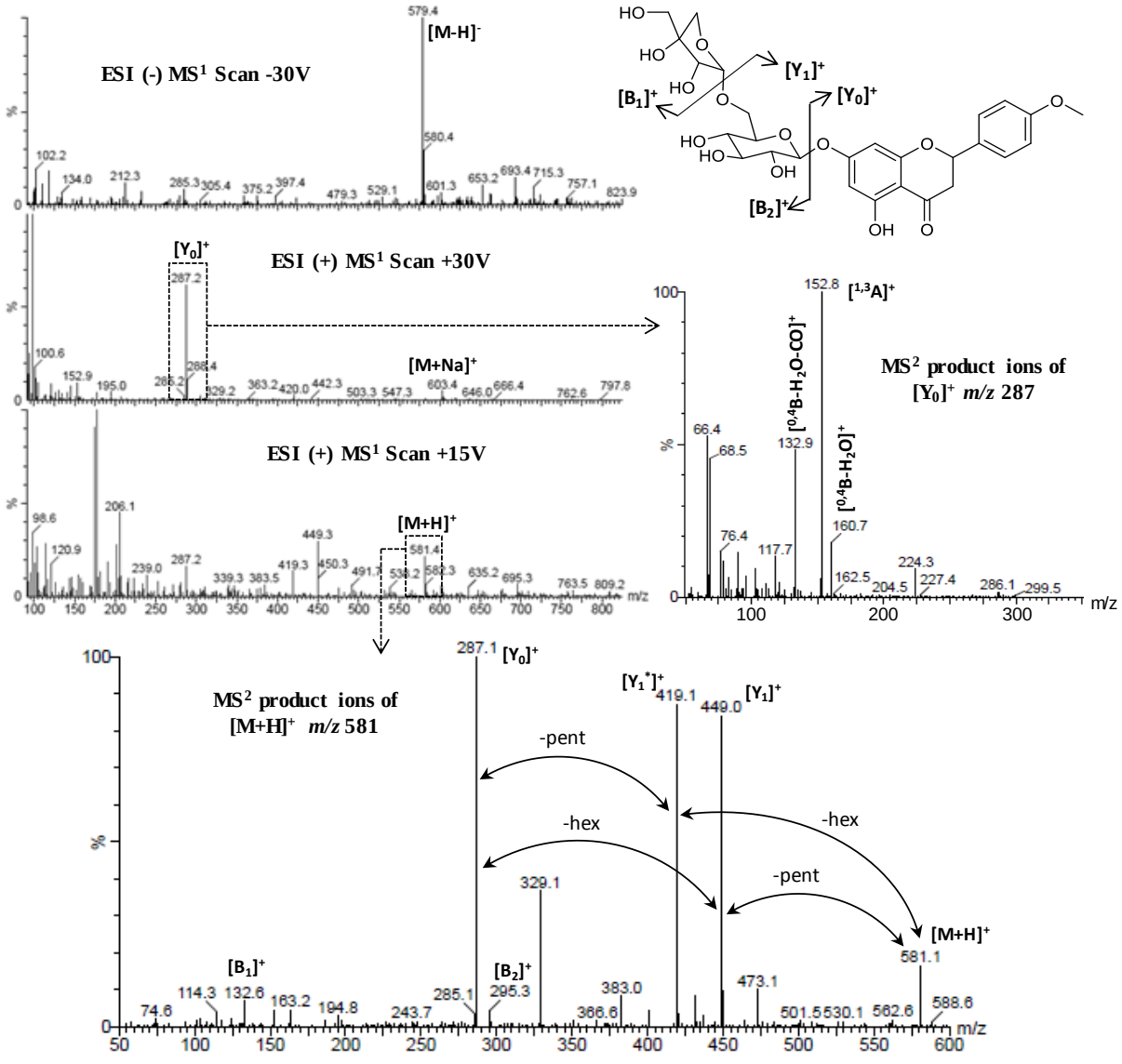

Fig. 1. Main fragmentation observed for protonated flavonoid-*O*-diglycosides and MS^1 and MS^2 data of isosakuranetin-7-*O*-apioglucoside.

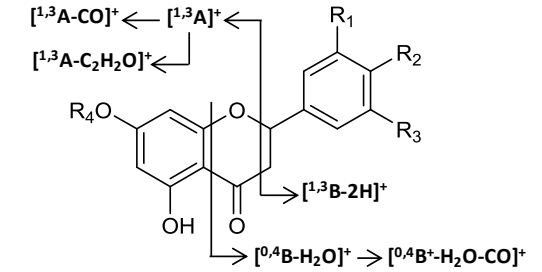

Peak	R_1	R_2	R_3	R_4
5	OH	OH	H	glc
6	OH	H	OH	api(1→6)glc
8	OH	OH	H	rut
13	H	OH	H	api(1→6)glc
15	OCH_3	OH	H	api(1→6)glc
19	OH	OCH_3	H	api(1→6)glc
27	H	OCH_3	H	api(1→6)glc
28	H	OH	H	H
29	H	OCH_3	H	rut

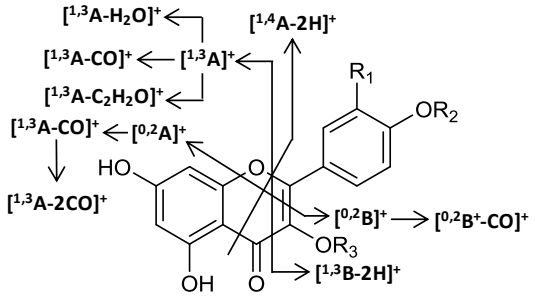

Peak	R_1	R_2	R_3
9	OH	glc	rut
20	OH	H	rut
25	H	H	glc
26	H	H	rut

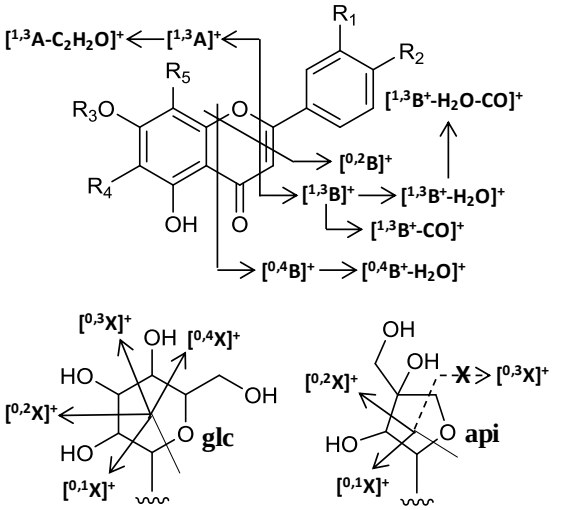

Peak	R_1	R_2	R_3	R_4	R_5
4	H	OH	H	glc	glc
7	H	OH	H	api	glc
11	H	OH	H	H	glc
14	H	OCH_3	H	glc	glc
16	H	OH	H	glc	api
17	H	OH	H	glc	H
18	OH	OH	api(1→6)glc	H	H
21	H	OH	H	api	api
22	H	OH	api(1→6)glc	H	H
23	H	OH	glc	H	H
24a	H	OH	rut	H	H
24b*	OCH_3	OH	api(1→6)glc	H	H
30	H	OCH_3	api(1→6)glc	H	H

*Could be the isomer diomestin

Fig. 2. Structures of the flavonoids present in the studied *Faramea* spp. and fragmentation pathways of the respective aglycones and sugar units of *C*-glycosides.

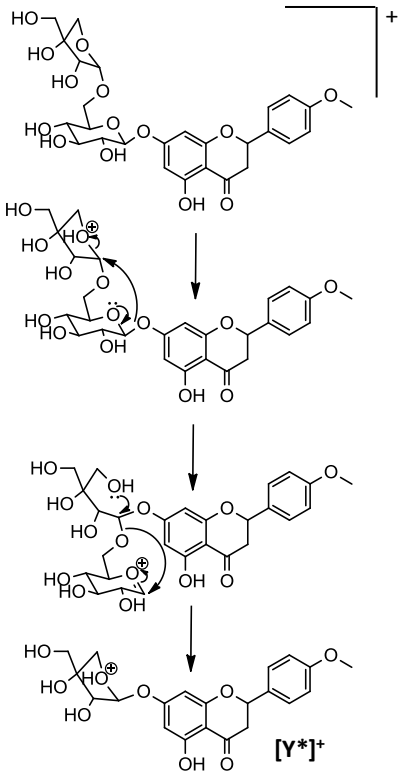

Fig. 3. Suggested MS fragmentation mechanism for the internal hexose loss.

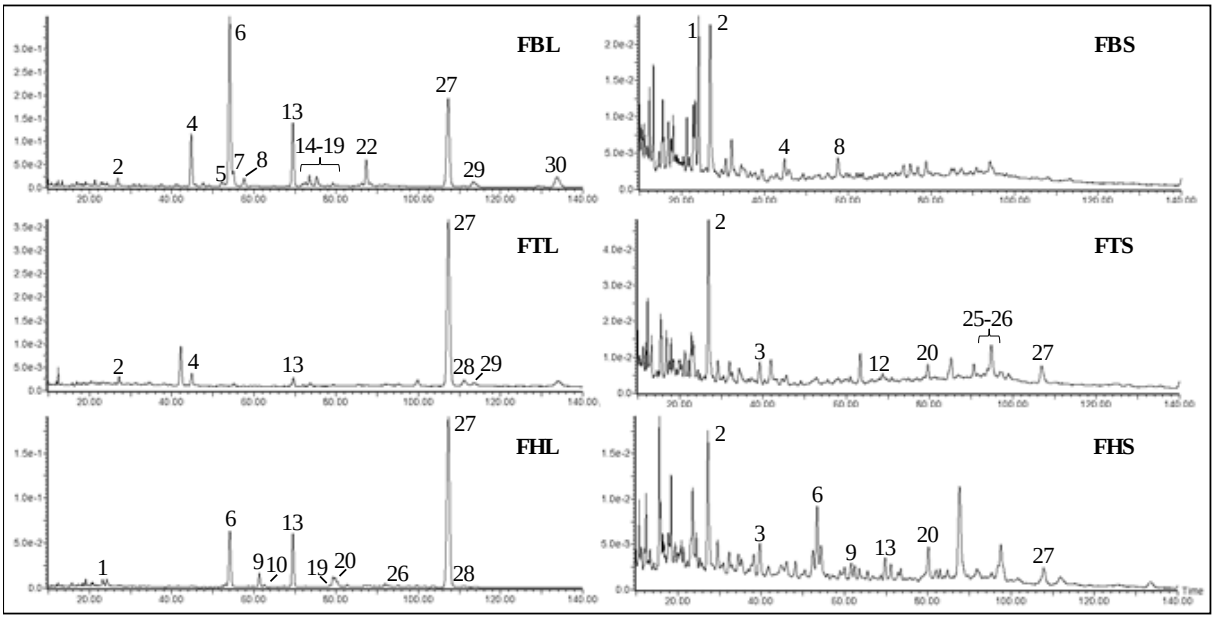

Fig. 4. HPLC-UV polyphenolic profiles at 280 nm of the leaf (L) and stem (S) MeOH extracts from *Faramea bahiensis* (FB), *Faramea truncata* (FT) and *Faramea hyacinthina* (FH).

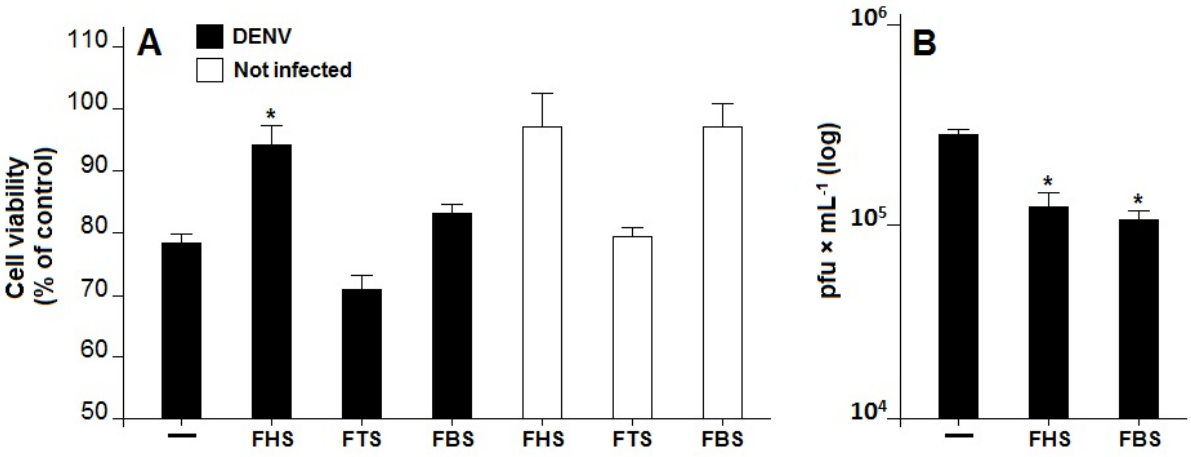

Fig. 5. Cell viability and antiviral effect of stem MeOH extracts from *Faramea bahiensis* (FBS), *Faramea hyacinthina* (FHS) and *Faramea truncata* (FTS). HepG2 cells were infected with DENV-2 16681 or not, and treated with 50 µg/ml of the *Faramea* extracts. (A) Cell viability was assessed by MTT assay 48 h post infection and results are expressed in % of control. Non-infected and treated conditions were used as control of cytotoxicity and cell proliferation (white bars). (B) Viral quantification in conditioned medium of culture by plaque assay. Symbol (-) is used for untreated conditions. *p<0,005.

Table 1. Polyphenolic composition of the leaf and stem MeOH extracts from *Faramea bahiensis*, *F. truncata* and *F. hyacinthina*

Peak	Compound	Class	Rt (min)	*F. bahiensis*		*F. truncata*		*F. hyacinthina*	
				Leaf	Stem	Leaf	Stem	Leaf	Stem
1	Caffeic acid	HCA	24.3	-	1.0	-	-	0.6	-
2	Syringic acid	HBA	26.9	0.5	0.8	0.1	1.7	-	0.9
3	Scopoletin	CM	39.8	-	-	-	0.6	-	0.4
4	Api-6,8-di-*C*-glc	FVN	44.7	6.0	0.3	0.3	-	-	-
5	Eri-7-*O*-glc	FVNN	52.3	0.5	-	-	-	-	-
6	5,3',5'-trihydroxyflavanone-7-*O*-api(1→6)glc	FVNN	54.1	25.2	-	-	-	8.3	0.5
7	Api-6-*C*-api-8-*C*-glc	FVN	55.0	1.2	-	-	-	-	-
8	Eri-7-*O*-rut	FVNN	57.6	1.1	0.3	-	-	-	-
9	Que-3-*O*-rut-4'-*O*-glc	FVL	61.3	-	-	-	-	3.2	0.2
10	Kaem-*O*-rut-*O*-glc	FVL	62.5	-	-	-	-	0.3	-
11	Api-8-*C*-glc	FVN	64.7	0.1	-	-	-	-	-
12	Kaem-*O*-rut-*O*-glc	FVL	68.8	-	-	-	0.2	-	-
13	Nar-7-O-api(1→6)glc	FVNN	69.5	8.2	-	0.3	-	7.2	0.2
14	Aca-6,8-di-*C*-glc	FVN	71.8	0.2	-	-	-	-	-
15	Heri-7-*O*-api(1→6)glc	FVNN	72.5	0.5	-	-	-	-	-
16	Api-6-*C*-glc-8-*C*-api	FVN	73.5	0.9	-	-	-	-	-
17	Api-6-*C*-glc	FVN	74.2	0.1	-	-	-	-	-
18	Lut-7-*O*-api(1→6)glc	FVN	75.2	1.2	-	-	-	-	-
19	Hes-7-*O*-api(1→6)glc	FVNN	79.2	0.4	-	-	-	1.3	-
20	Que-3-*O*-rut	FVL	79.6	-	-	-	0.5	3.2	0.8
21	Api-6,8-di-*C*-api	FVN	86.2	0.3	-	-	-	-	-
22	Api-7-*O*-api(1→6)glc	FVN	87.3	3.7	-	-	-	-	-
23	Api-7-*O*-glc	FVN	88.4	0.4	-	-	-	-	-
24a	Api-7-*O*-rut	FVN	90.5	0.2**	-	-	-	-	-
24b	Chry/Dio-7-*O*-api(1→6)glc	FVN	90.5	0.2**	-	-	-	-	-
25	Kaem-3-*O*-glc	FVL	93.5	-	-	-	0.1	-	-
26	Kaem-3-*O*-rut	FVL	94.8	-	-	0.1	1.1	0.5	0.1
27	Isk-7-*O*-api(1→6)glc	FVNN	107.3	18.1	-	9.4	0.5	38.2	0.4
28	Nar	FVNN	111.0	0.3	-	0.3	-	0.2	-
29	Isk-7-*O*-rut	FVNN	113.4	1.5	-	0.1	-	-	-
30	Aca-7-*O*-api(1→6)glc	FVN	133.8	3.9	-	-	-	-	-

*concentration in mg/g of dry extract. **concentration relative to compounds **24a** and **24b**

References

Abad-Garcia, B., Berrueta, L. A., Garmon-Lobato, S., Gallo, B., Vicente, F., 2009. A general analytical strategy for the characterization of phenolic compounds in fruit juices by high-performance liquid chromatography with diode array detection coupled to electrospray ionization and triple quadrupole mass spectrometry. J. Chromatogr. A 1216, 5398-5415.

Abad-Garcia, B., Garmon-Lobato, S., Berrueta, L. A., Gallo, B., Vicente, F., 2008. New features on the fragmentation and differentiation of *C*-glycosidic flavone isomers by positive electrospray ionization and triple quadrupole mass spectrometry. Rapid Commun. Mass Spectrom. 22, 1834-1842.

Abu-Reidah, I. M., Arráez-Román, D., Quirantes-Piném, R., Fernández-Arroyo, S., Segura-Carretero, A., Fernández-Gutiérrez, A., 2012. HPLC-ESI-Q-TOF-MS for a comprehensive characterization of bioactive phenolic compounds in cucumber whole fruit extract. Food Res. Int. 46, 108-117.

Barboza, R. S., Valente, L. M. M., Wolff, T., Assunção-Miranda, I., Neris, R. S. L., Guimarães-Andrade, I. P., Gomes, M., 2017. Antiviral activity of *Faramea hyacinthina* and *Faramea truncata* leaves on dengue virus type-2 and their major compounds. Unpublished results.

Brazilian-Federal-Government, 2017. Monitoramento dos casos de dengue, febre de chikungunya e febre pelo vírus Zika até a Semana Epidemiológica 12. Secretaria de Vigilância em Saúde, Boletim Epidemiológico 48, vol. 48, pp. 1-10.

Bucar, F., Ninov, S., Ionkova, I., Kartnig, T., Schubert-Zsilavecz, M., Asenov, I., Konuklugil, B., 1988. Flavonoids from *Phlomis nissolii*. Phytochemistry 48, 573-575.

Çalis, I., Güvenç, A., Armagan, M., Koyuncu, M., Gotfredsen, C. H., Jensen, S. R., 2008. Secondary metabolites from *Eremostachys laciniata*. Nat. Prod. Commun. 3, 117-124.

Cao, J., Xia, X., Dai, X., Xiao, J., Wang, Q., Andrae-Marobela, K., Okatch, H., 2013. Flavonoids profiles, antioxidant, acetylcholinesterase inhibition activities of extract from *Dryoathyrium boryanum* (Willd.) Ching. Food Chem. Toxicol. 55, 121-128.

Cavaliere, C., Foglia, P., Pastorini, E., Samperi, R., Laganà, A., 2005. Identification and mass spectrometric characterization of glycosylated flavonoids in *Triticum durum* plants by high-performance liquid chromatography with tandem mass spectrometry. Rapid Commun. Mass Espectrom. 19, 3143-3158.

Chicca, A., Tebano, M., Adinolfi, B., Ertugrul, K., Flamini, G., Nieri, P., 2011. Anti-proliferative activity of aguerin B and a new rare *nor*-guaianolide lactone isolated from the aerial parts of *Centaurea deflexa*. Eur. J. Med. Chem. 46, 3066-3070.

Domon, B., Costello, C. E., 1988. Structure elucidation of glycosphingolipids and gangliosides using high-performance tandem mass spectrometry. Biochem. 27, 1534-1543.

Farooq, M. O., Gupta, S. R., Kiamuddin, M., Rahman, W., Seshadri, T. R., 1953. Chemical examination of cerelry seeds. J. Sci. Indust. Res. 12B, 400-407.

Ferreres, F., Gil-Izquierdo, A., Andrade, P. B., Valentão, P., Tomás-Barberán, F. A., 2007. Characterization of *C*-glycosyl flavones *O*-glycosylated by liquid chromatography-tandem mass spectrometry. J. Chromatogr. A 1161, 214-223.

Ferreres, F., Silva, B. M., Andrade, P. B., Seabra, R. M., Ferreira, M. A., 2003. Approach to the study of *C*-glycosyl flavones by ion trap HPLC-PAD-ESI/MS/MS: application to seeds of quince (*Cydonia oblonga*). Phytochem. Anal. 14, 352-359.

Gil-Izquierdo, A., Riquelme, M. T., Porras, N., Ferreres, F., 2004. Effect of the rootstock and interstock grafted in lemon tree (*Citrus limon* (L.) Burm.) on the flavonoid content of lemon juice. J. Agric. Food Chem. 52, 324-331.

Guo, C., Zhou, Z., Wen, Z., Liu, Y., Zeng, C., Xiao, D., Ou, M., Han, Y., Huang, S., Liu, D., Ye, X., Zou, X., Wu, J., Wang, H., Zeng, E. Y., Jing, C., Yang, G., 2017. Global epidemiology of Dengue outbreaks in 1990–2015: A systematic review and meta-analysis. Front. Cell. Infect. Microbiol. 7:317, 1-11.

Hori, K., Satake, T., Saiki, Y., Tanaka, N., Murakami, T., Cheng, C., 1988. Chemical and chemotaxonomical stuidies of Filices. LXXIV. The novel flavanones glycosides of *Pyrrosia linearfolia* (Hook.) Ching. Yakugaku Zasshi 108, 417-421.

Jardim, J. G., Zappi, D. C., 2008. Two new species of *Faramea* (Rubiaceae, Coussareeae) from Eastern Brazil. Novon 18, 67-71.

Jay, M., Viricel, M., Gonnetm, J. F., 2006. Flavonoids Chemistry, Biochemistry and Applications. CRC Press, Boca Raton.

Kaneko, T., Sakamoto, M., Ohtani, K., Ito, A., Kasai, R., Yamasaki, K., Padorina, W. G., 1995. Secoiridoid and flavonoid glycosides from *Gonocaryum calleryanum*. Phytochemistry 39, 115-120.

Khattab, A. A., Nada, S. A., 2007. Flavonoids from *Montanoa bipinnatifida* leaves and evaluation of hepatoprotective activity of extract. Bull. Fac. Pharm. Cairo Univ. 45, 181-185.

La, M., Zhang, F., Gao, S., Liu, X., Wu, Z., Sun, L., Tao, X., Chen, W., 2015. Constituent analysis and quality control of *Lamiophlomis rotata* by LC-TOF/MS and HPLC-UV. J. Pharm. Biomed. Anal. 102, 366-376.

Li, Y., Li, J., Wang, N., Yao, X., 2008. Flavonoids and a new polyacetylene from *Bidens parviflora* Willd. Molecules 13, 1931-1941.

Ma, Y. L., Li, Q. M., Van den Heuvel, H., Claeys, M., 1997. Characterization of flavone and flavonol aglycones by collision-induced dissociation tandem mass spectrometry. Rapid Commun. Mass Spectrom. 11, 1357-1364.

Ma, Y. L., Vedernikova, I., Van den Heuvel, H., Claeys, M., 2000. Internal glucose residue loss in protonated *O*-diglycosyl flavonoids upon low-energy collision-induced dissociation. J. Am. Soc. Mass Spectrom. 11, 136-144.

March, R. E., Lewars, E. G., Stadey, C. J., Miao, X. S., Zhao, X. M., Metcalfe, C. D., 2006. A comparison of flavonoid glycosides by electrospray tandem mass spectrometry. Int. J. Mass Spectrom. 248, 61-85.

Markham, K. R., 1982. Techniques of flavonoid identification. Academic Press, London.

Masuoka, C., Ono, M., Yasuyuki, I., Nohara, T., 2003. Antioxidative, antiyaluronidase and antityrosinase activities od some constituents from the aerial part of *Piper elongatum* Vahl. Food Sci. Technol. Res. 9, 197-201.

Nascimento, A. C., Valente, L. M. M., Gomes, M., Barboza, R. S., Wolff, T., Neris, R. L. S., Figueiredo, C. M., Assunção-Miranda, I., 2017. Antiviral activity of *Faramea bahiensis* leaves on dengue virus type-2 and characterization of a new antiviral flavanone glycoside. Phytochem. Lett. 19, 220-225.

Picerno, P., Mencherini, T., Lauro, M. R., Barbato, F., Aquino, R., 2003. Phenolic constituents and antioxidant properties of *Xanthosoma violaceum* leaves. J. Agric. Food Chem. 51, 6423-6428.

Siciliajo, T., De Tommasi, N., Morelli, I., Braca, A., 2004. Study of flavonoids of *Sechium edule* (Jacq) Swartz (Cucurbitaceae) different edible organs by liquid chromatography photodiode array mass spectrometry. J. Agric. Food Chem. 52, 6510-6515.

Takahashi, H., Hirata, S., Minami, H., Fukuyama, Y., 2001. Triterpene and flavanone glycoside from *Rhododendron simsii*. Phytochemistry 56, 875-879.

Wanjala, C. C. W., Majinda, R. R. T., 1999. Flavonoid glycosides from *Crotalaria podocarpa*. Phytochemistry 51, 705-707.

Waridel, P., Wolfender, J. L., Ndjoko, K., Hobby, K. R., Major, H. J., Hostettmann, K., 2001. Evaluation of quadrupole time-of-flight tandem mass spectrometry and ion-trap multiple-stage mass spectrometry for the differentiation of *C*-glycosidic flavonoid isomers. J. Chromatogr. A 926, 29-41.

WHO, Updated in April 2017. Dengue and severe dengue. Fact sheet 117.

Zhang, Z., ElSohly, H. N., Li, X.-C., Khan, S. I., Broedel, S. E., Raulli-Jr, R. E., Cihlar, R. L., Walker, L. A., 2003. Flavanone glycosides from *Miconia trailii*. J. Nat. Prod. 66, 39-41.

Table 1. Polyphenolic composition of the leaf and stem MeOH extracts from *Faramea bahiensis*, *F. truncata* and *F. hyacinthina*

Peak	Compound	Class	R_t (min)	*F. bahiensis*		*F. truncata*		*F. hyacinthina*	
				Leaf	Stem	Leaf	Stem	Leaf	Stem
1	Caffeic acid	HCA	24.3	-	1.0	-	-	0.6	-
2	Syringic acid	HBA	26.9	0.5	0.8	0.1	1.7	-	0.9
3	Scopoletin	CM	39.8	-	-	-	0.6	-	0.4
4	Api-6,8-di-*C*-glc	FVN	44.7	6.0	0.3	0.3	-	-	-
5	Eri-7-*O*-glc	FVNN	52.3	0.5	-	-	-	-	-
6	5,3',5'-trihydroxyflavanone-7-*O*-api(1→6)glc	FVNN	54.1	25.2	-	-	-	8.3	0.5
7	Api-6-*C*-api-8-*C*-glc	FVN	55.0	1.2	-	-	-	-	-
8	Eri-7-*O*-rut	FVNN	57.6	1.1	0.3	-	-	-	-
9	Que-3-*O*-rut-4'-*O*-glc	FVL	61.3	-	-	-	-	3.2	0.2
10	Kaem-*O*-rut-*O*-glc	FVL	62.5	-	-	-	-	0.3	-
11	Api-8-*C*-glc	FVN	64.7	0.1	-	-	-	-	-
12	Kaem-*O*-rut-*O*-glc	FVL	68.8	-	-	-	0.2	-	-
13	Nar-7-O-api(1→6)glc	FVNN	69.5	8.2	-	0.3	-	7.2	0.2
14	Aca-6,8-di-*C*-glc	FVN	71.8	0.2	-	-	-	-	-
15	Heri-7-*O*-api(1→6)glc	FVNN	72.5	0.5	-	-	-	-	-
16	Api-6-*C*-glc-8-*C*-api	FVN	73.5	0.9	-	-	-	-	-
17	Api-6-*C*-glc	FVN	74.2	0.1	-	-	-	-	-
18	Lut-7-*O*-api(1→6)glc	FVN	75.2	1.2	-	-	-	-	-
19	Hes-7-*O*-api(1→6)glc	FVNN	79.2	0.4	-	-	-	1.3	-
20	Que-3-*O*-rut	FVL	79.6	-	-	-	0.5	3.2	0.8
21	Api-6,8-di-*C*-api	FVN	86.2	0.3	-	-	-	-	-
22	Api-7-*O*-api(1→6)glc	FVN	87.3	3.7	-	-	-	-	-
23	Api-7-*O*-glc	FVN	88.4	0.4	-	-	-	-	-
24a	Api-7-*O*-rut	FVN	90.5	0.2**	-	-	-	-	-
24b	Chry/Dio-7-*O*-api(1→6)glc	FVN	90.5	0.2**	-	-	-	-	-
25	Kaem-3-*O*-glc	FVL	93.5	-	-	-	0.1	-	-
26	Kaem-3-*O*-rut	FVL	94.8	-	-	0.1	1.1	0.5	0.1
27	Isk-7-*O*-api(1→6)glc	FVNN	107.3	18.1	-	9.4	0.5	38.2	0.4
28	Nar	FVNN	111.0	0.3	-	0.3	-	0.2	-
29	Isk-7-*O*-rut	FVNN	113.4	1.5	-	0.1	-	-	-
30	Aca-7-*O*-api(1→6)glc	FVN	133.8	3.9	-	-	-	-	-

*concentration in mg/g of dry extract. **concentration relative to compounds **24a** and **24b**

Figure 1

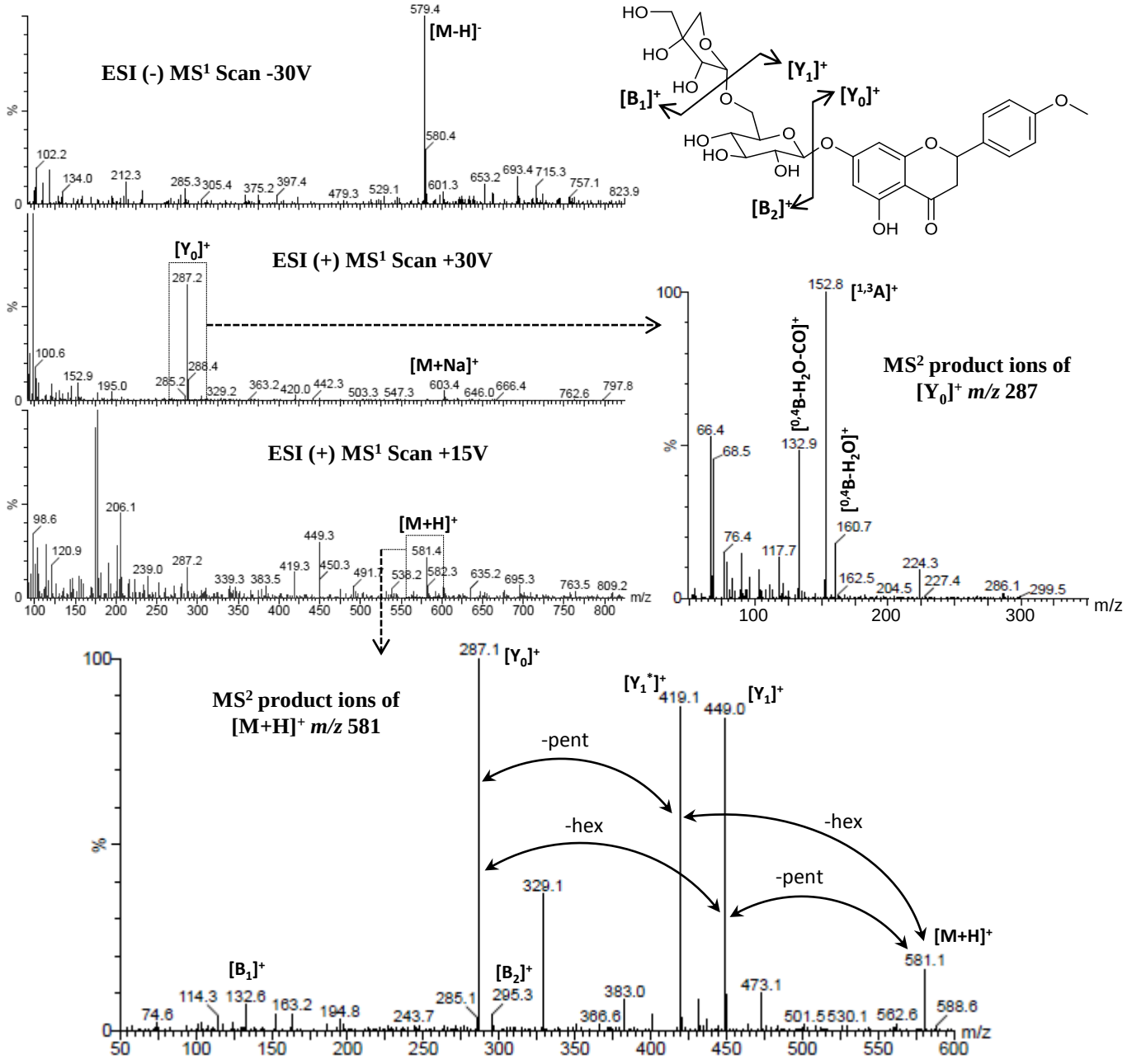

Wolff et al. Figure 1

Figure 2

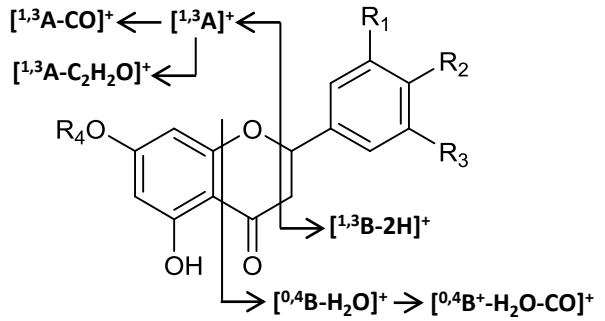

Peak	R_1	R_2	R_3	R_4
5	OH	OH	H	glc
6	OH	H	OH	api(1→6)glc
8	OH	OH	H	rut
13	H	OH	H	api(1→6)glc
15	OCH_3	OH	H	api(1→6)glc
19	OH	OCH_3	H	api(1→6)glc
27	H	OCH_3	H	api(1→6)glc
28	H	OH	H	H
29	H	OCH_3	H	rut

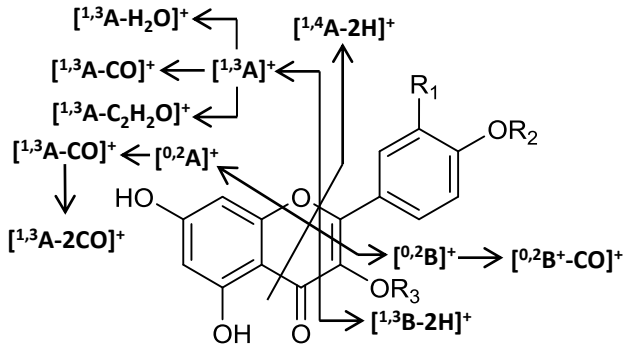

Peak	R_1	R_2	R_3
9	OH	glc	rut
20	OH	H	rut
25	H	H	glc
26	H	H	rut

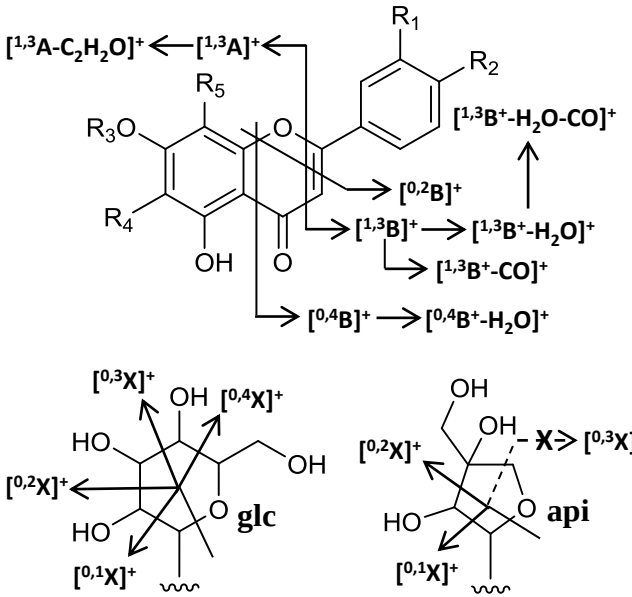

Peak	R_1	R_2	R_3	R_4	R_5
4	H	OH	H	glc	glc
7	H	OH	H	api	glc
11	H	OH	H	H	glc
14	H	OCH_3	H	glc	glc
16	H	OH	H	glc	api
17	H	OH	H	glc	H
18	OH	OH	api(1→6)glc	H	H
21	H	OH	H	api	api
22	H	OH	api(1→6)glc	H	H
23	H	OH	glc	H	H
24a	H	OH	rut	H	H
24b*	OCH_3	OH	api(1→6)glc	H	H
30	H	OCH_3	api(1→6)glc	H	H

*Could be the isomer diomestin

Wolff et al. Figure 2

Figure 3

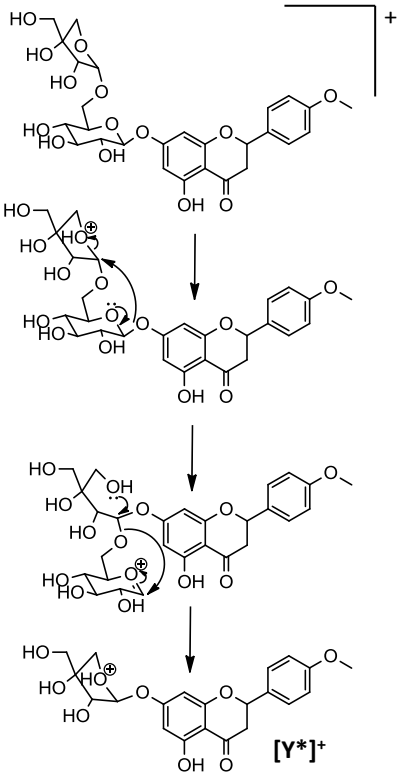

Wolff et al. Figure 3

Figure 4

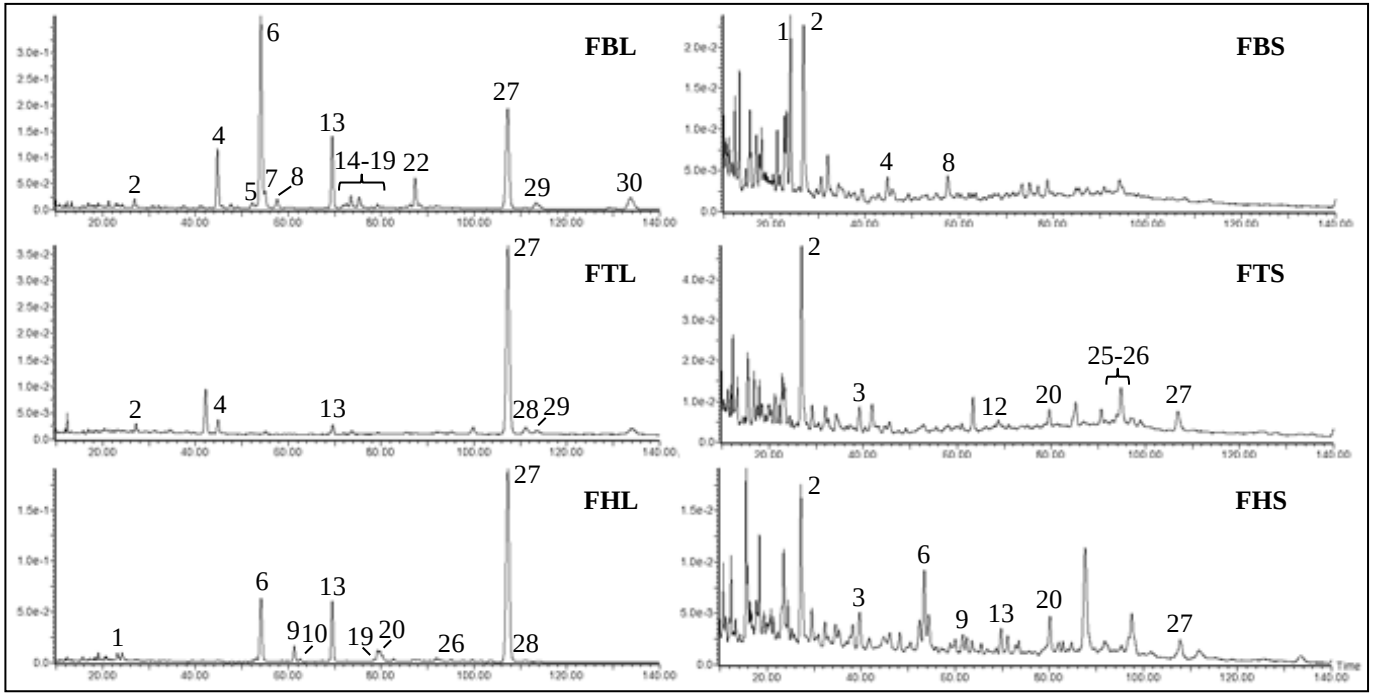

Wolff et al. Figure 4.

Figure 5

Click here to download high resolution image

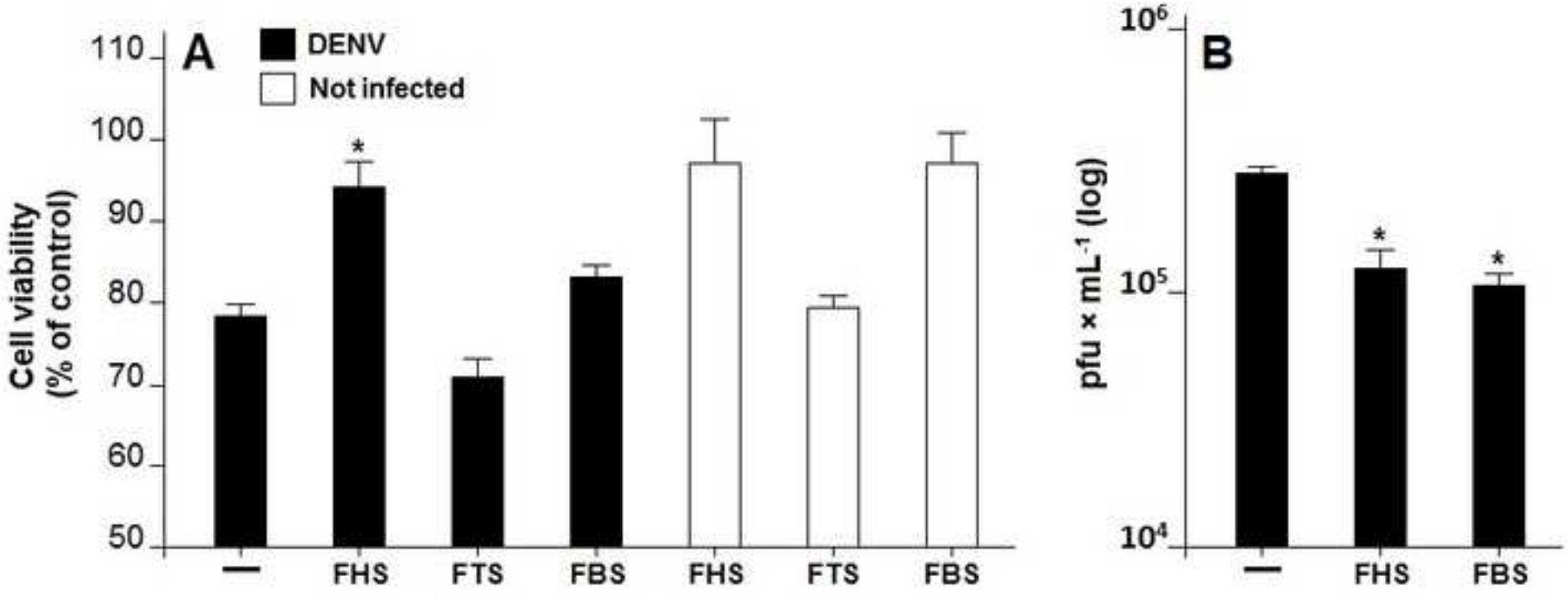

Wolff et al.

Comprehensive characterization of polyphenols in leaves and stems of three anti-DENV-2 active Brazilian *Faramea* species (Rubiaceae) by HPLC-DAD-ESI-CID-MS/MS

Figure captions

Fig. 1. Main fragmentation observed for protonated flavonoid-*O*-diglycosides and MS^1 and MS^2 data of isosakuranetin-7-*O*-apioglucoside.

Fig. 2. Structures of the flavonoids present in the studied *Faramea* spp. and fragmentation pathways of the respective aglycones and sugar units of *C*-glycosides.

Fig. 3. Suggested MS fragmentation mechanism for the internal hexose loss.

Fig. 4. HPLC-UV polyphenolic profiles at 280 nm of the leaf (L) and stem (S) MeOH extracts from *Faramea bahiensis* (FB), *Faramea truncata* (FT) and *Faramea hyacinthina* (FH).

Fig. 5. Cell viability and antiviral effect of stem MeOH extracts from *Faramea bahiensis* (FBS), *Faramea hyacinthina* (FHS) and *Faramea truncata* (FTS). HepG2 cells were infected with DENV-2 16681 or not, and treated with 50 µg/ml of the *Faramea* extracts. (A) Cell viability was assessed by MTT assay 48 h post infection and results are expressed in % of control. Non-infected and treated conditions were used as control of citotoxicity and cell proliferation (white bars). (B) Viral quantification in conditioned medium of culture by plaque assay. Symbol (-) is used for untreated conditions. *p<0,005.